

Estimating safety factor for femoral plates subjected to in vivo loads

Original

Estimating safety factor for femoral plates subjected to in vivo loads / Bologna, F.A., Audenino, A., Terzini, M.. - In: CURRENT DIRECTIONS IN BIOMEDICAL ENGINEERING. - ISSN 2364-5504. - 10 (4):(2024), pp. 103-106. (58th Annual Conference of the German Society for Biomedical Engineering Stuttgart (DEU) 18 – 20 September 2024) [10.1515/cdbme-2024-2025].

Availability:

This version is available at: 11583/2997812 since: 2025-02-24T18:01:05Z

Publisher:

Walter de Gruyter

Published

DOI:10.1515/cdbme-2024-2025

Terms of use:

This article is made available under terms and conditions as specified in the corresponding bibliographic description in the repository

Publisher copyright

(Article begins on next page)

Federico Andrea Bologna*, Alberto Luigi Audenino and Mara Terzini

Estimating safety factor for femoral plates subjected to *in vivo* loads

An *in silico* framework for regulatory testing

<https://doi.org/10.1515/cdbme-2024-2025>

Abstract: Fatigue behaviour is a crucial aspect of mandatory mechanical tests for regulatory purposes, aimed at determining the load at which the bone plate withstands under a specific number of cycles, known as the *runout* condition. However, current test standards, such as ASTM F382, provide setup configurations without explicit guidelines on required fatigue strength. The determination of the minimum level of *in vivo* performance that the plate must fulfil remains an open issue, which is frequently addressed by the direct comparison with predicate devices. To address this gap, this study proposes an *in silico* framework to estimate maximum stress on implanted femoral plates for comparison with four-point bending tests described in the ASTM standard, deriving appropriate safety factors. As case studies, three femoral plates were assessed, and results showed safety factors above 1.1, indicating the reliability of the implanted plates.

Keywords: Osteosynthesis device testing, ASTM F382, four-point bending, implanted plate, safety factor.

1 Introduction

Despite advancements in the design of modern bone plates, implant failures still occur due to fatigue fractures induced by cyclic loading. Understanding the endurance of bone plates, particularly those used in lower extremity applications exposed to cyclic ambulatory loading, is crucial. Fatigue behaviour is a pivotal aspect of mandatory mechanical tests for regulatory purposes, which aim to determine the load at which the plate withstands under a specific number of cycles, known as the *runout* condition. The current test standards, such as ASTM F382 [1], only provide the setup configuration without furnishing explicit guidelines regarding the required fatigue

strength of the bone plate in the *runout* condition. The Food and Drug Administration (FDA) recently issued the first criteria for quantifying plate performance [2]. Again, this guideline refers only to static tests and does not include any indication regarding plate endurance.

In this context, several studies have focused on the test condition, neglecting the loads that occur *in vivo*. Indeed, *in silico* methodologies have been used to determine the stress distributions on generic bone plates under four-point bending in order to evaluate different designs [3] or the effect of thread removal and screw hole offsetting [4]. On the contrary, other studies focused on the post-surgical conditions that led to implant failure by subjecting the plate to the loads present *in vivo*. Few examples are the work of [5], where unconventional loading situations, such as those caused by stumbling and in the presence of incomplete bone healing, were statically evaluated in a periprosthetic femur plate system, and the work of [6], which performed a failure analysis on a humeral plate exploring various loading scenarios through finite element (FE) analysis to investigate the mechanism that led to the failure of the plate. In this latter, the fatigue assessments were conducted by inputting the obtained values of maximum equivalent stress into a commercial software to estimate the number of cycles based on the loading condition using theoretical fatigue criteria. Other basic fatigue assessments can be found in [7] where FE analysis was used to investigate the fatigue characteristics of hybrid reconstruction plates intended for the treatment of segmental defects of the mandible, employing conventional S-N curves (stress amplitude vs. number of cycles to failure). The determination of the minimum level of *in vivo* performance and related fatigue life that the plate must fulfil remains an open issue [8, 9], which is frequently addressed through direct comparison with predicate devices. To the authors' knowledge, no study has compared the test conditions described by the ASTM standard with the conditions to which the plate will be subjected once implanted.

To address these challenges, the present work proposes an *in silico* framework to estimate the maximum stress on implanted femoral plates for comparison with that obtained from four-point bending tests according to ASTM F382 standards, thereby deriving appropriate safety factors.

*Corresponding author: Federico Andrea Bologna: Politecnico di Torino, Turin, Italy, e-mail: federico.bologna@polito.it
Alberto Luigi Audenino, Mara Terzini: Politecnico di Torino, Turin, Italy

2 Materials and Methods

Three different femoral plates were assessed in the present study. *Plate01* and *Plate02* are distal plates, while *Plate03* is a diaphyseal plate. Table 1 lists their material, the static ultimate tensile strength (σ_{UTS}), and anatomical location.

Table 1: Femoral plates involved in the study and their main characteristics.

Plate	Material	σ_{UTS} (MPa)	Femoral Region
01	Stainless Steel	986	Distal
02	Ti6Al4V	968	Distal
03	Pure Titanium	991	Diaphyseal

2.1 Four-Point Bending Test

For each bone plate, a FE model of the experimental setup according to ASTM F382 (Figure 1) was realised in Ansys

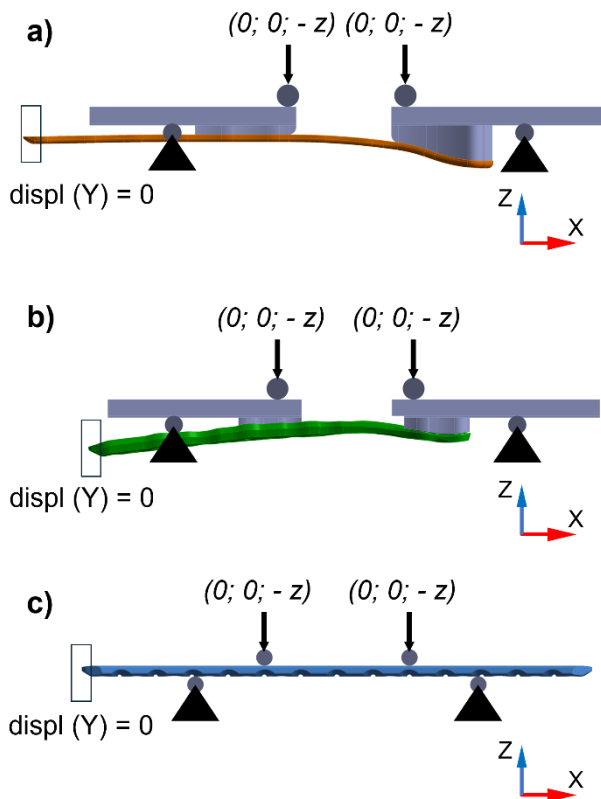


Figure 1: FE model of a) *Plate01*, b) *Plate02*, and c) *Plate03* in the four-point bending configuration. Black arrows represent the imposed displacements, while black triangles represent fixed supports.

Mechanical 2022 R2 (Ansys Inc., Canonsburg, USA). Extension segments made of AISI 630 were adopted for plates that did not directly fit into the test configuration, ensuring a sufficiently long section of symmetry. The rollers were modelled as rigid cylinders, while the plates and extensions were assumed to be linear elastic. The Young's modulus was assumed to be 100 GPa for titanium plates and 200 GPa for steel plates and extensions. A second-order tetrahedral mesh was created for each plate with a dimension of 1 mm. Refinements up to 0.2 mm have been evaluated in the working length of the plate to assess the correct convergence of the model. A vertical displacement (z) was applied at the centre of the two loading rollers and rigidly transferred to their cylindrical surface to replicate the experimental test. This displacement was adjusted for each plate to slightly exceed the yield point, ensuring full engagement of the linear field. While the support rollers were considered as fixed supports, a constraint along the y -axis was applied at one end of the plate, away from the working length, to prevent frontal sliding. The contact between the plate and the rollers was assumed to be frictionless.

For each simulation, the time step corresponding to the experimental runout load (L) described in [8] was identified, and the maximum stress in the working length was calculated at that point. The FE analyses were performed by using the Ansys Mechanical APDL (Ansys Inc., Canonsburg, USA) implicit solver on twelve computing cores of a workstation equipped with Intel® Core™ i7-12700 and 32 GB RAM.

2.2 Femur-Plate Implant

The FE model (Ansys Inc., Canonsburg, USA) of each femur-plate construct was created by positioning the plate in the anatomical site for which it was designed. The femur was modelled with cortical bone only, and the plate was fixed to the bone through the two holes adjacent to the free hole (Figure 2). The bone callus elements were assigned an elastic modulus equal to 6% of the femoral cortical bone [10]. Two bi-cortical screws were modelled with rigid elements in order to fix each plate. The distal end of the femur was constrained in all degrees of freedom [11] and loads measured during normal walking were applied to the femur assuming a body mass of 100 kg [12]. The reaction force acting on the femoral head and the muscle forces were applied as a ramp to reach their maximum values (corresponding to 45% of the step cycle) [13]. Loads were distributed over the femoral head and the greater trochanter using rigid elements. While a second-order tetrahedral mesh with a size of 1 mm and a refinement of 0.2 mm in working length was generated for the plate, as well as in the four-point bending condition, the femoral bone was

meshed using a regular second-order tetrahedral mesh with an average edge length of 2 mm.

Therefore, the simulation was repeated for the three femoral plates, placing the bone callus at the level of each hole, and repeating the operation for all holes along the working length of the plate. The position of the screws was adjusted accordingly to leave only one hole free at a time.

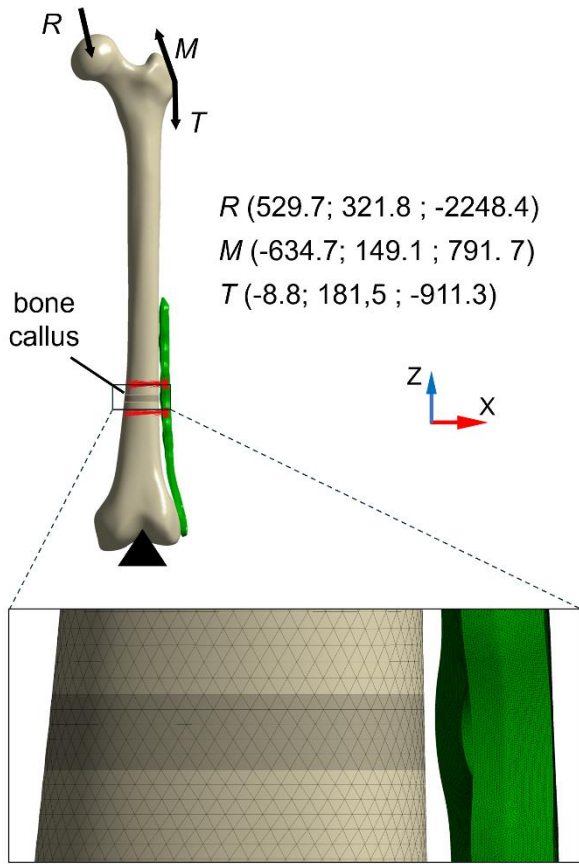


Figure 2: Finite element model of the bone-plate construct (*Plate02*). The rigid elements used to model the screws are depicted in red. The femoral portion in dark grey represents the bone callus. A zoomed-in view of the mesh in the area around the critical hole is shown.

3 Results

In the four-point bending condition, *Plate03* appeared the most critical, as it showed peaks of tension around 800 MPa at the central holes. Regarding the results of the simulations conducted for the femur-plate construct, it emerged that the most critical region corresponded to the diaphyseal holes. Specifically, *Plate01* had shown a higher stress value ($\sigma_{max} = 590.2$ MPa) for the simulation with the first proximal free hole along the working length, as well as *Plate02* ($\sigma_{max} = 493.8$

MPa). *Plate03* consisted of six holes along the working length, three proximal and three distal, delimited by a central area of solid material. In this case, the hole with the highest stress ($\sigma_{max} = 501.4$ MPa) was the first distal one (Figure 3). Finally, the safety factors (SF) were calculated (Table 2). All plates show SFs greater than 1.1.

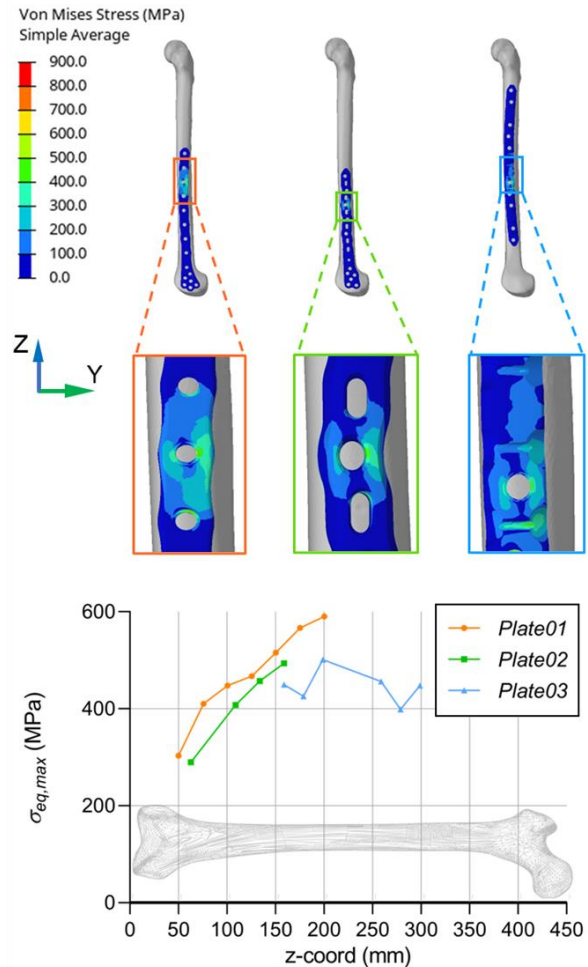


Figure 3: (Top) Distribution of equivalent stresses (von Mises) in the most critical hole for the three implants, namely *Plate01* on the left, *Plate02* in the centre, and *Plate03* on the right. A zoomed-in view of the critical region is provided for each plate. (Bottom) maximum equivalent stress in the most critical hole for the three plates as a function of the longitudinal coordinate (z) of the femur.

Table 2: Maximum equivalent stress (von Mises) in the most critical holes for four-point bending test (*4-pb*) and implanted condition (*impl*) and resulting safety factor (SF).

Plate	$\sigma_{max, 4-pb}$ (MPa)	$\sigma_{max, impl}$ (MPa)	SF
01	671.3	590.2	1.14
02	709.4	493.8	1.44
03	811.7	501.4	1.62

4 Discussion

In this work, an *in silico* framework was implemented to establish a rationale for the regulatory process of femoral osteosynthesis plates, providing valuable insights into the safety and reliability of implanted plates.

The four-point bending setup of a previously conducted experimental evaluation [8] was first replicated in the FE environment to assess the plates in an implanted condition. In *Plate03*, the maximum stress exceeded the yield limit, approaching the ultimate strength of the plate material, which was lower than that reported by Muthusamy *et al.* (2022) for the highest-performing design [4]. In the work of Muthusamy, the titanium alloy composing the bone plate was similar to that of *Plate03* (927 MPa vs. 991 MPa), as well as the thickness (5.05 mm vs. 5.12 mm), although the moment of inertia for the section with the hole was not specified. Nevertheless, the high stress remained localized around the screw hole. Runout under these conditions might occur where local yielding is adequately minute, allowing the material to undergo deformation that leads the yielding to cease [8]. Moreover, the choice to adopt an elastic material was made in the absence of the effective elasto-plastic curve of the material.

In the implanted plate condition, the maximum stresses were consistent with the theoretical formulation of Pauwels as reported by [14], showing that maximum stress on the femoral bone is highest at the greater trochanter and gradually decreased towards the condylar region.

Conservative assumptions as the employment of elements with a constant Young's modulus to represent the bony callus and the application of an over-constrained boundary condition at the distal end of the femur were adopted in the FE model of the implanted plate. Despite these simplifications, which likely led to an overestimation of the actual stress distribution, the calculated safety factors (SFs) on the maximum equivalent stress with respect to the test condition described by the ASTM standard were still greater than 1.1.

Future research will primarily aim to validate the FE model of the implanted plate to ensure its credibility. The investigated bone plate will be fixed to a composite femur to analyse the deformation field of the construct. Subsequently, enhancements to the *in silico* model of the implanted plate will be proposed to achieve a more accurate representation of the *in vivo* condition. Additionally, detailed modelling of the bone callus will be undertaken to evaluate stress reduction on the plate due to callus growth.

Furthermore, while this study focused solely on evaluating the femoral bone, the methodology can be extended to assess plates implanted in any anatomical region once the *in vivo* loads are identified. Multibody analyses of the human body can provide valuable insights into the loads experienced by fractured bones post-implantation of the plate [15].

In conclusion, this study enabled the assessment of maximum stress on a femoral plate through *in silico* methods to predict its *in vivo* performance. The evaluation relied on loads obtained experimentally using the test setup outlined in the ASTM F382 standard, defining a minimum level of *in vivo* performance and thus avoiding the need for experimental comparison with a predicate device.

Author Statement

Research funding: The authors state no funding involved.

Conflict of interest: Authors state no conflict of interest.

References

- [1] ASTM International. Standard Specification and Test Method for Metallic Bone Plates F382-99. West Conshohocken, USA; 2017.
- [2] Food and Drug Administration. Orthopedic Fracture Fixation Plates – Performance Criteria for Safety and Performance Based Pathway - Guidance for Industry and Food and Drug Administration Staff. Rockville, USA; 2022.
- [3] Drátovská V, Sedláček R, Padovec Z, Růžička P, Kratochvíl A. The mechanical properties and fatigue prediction of a new generation of osteosynthesis devices. *Strojnícky časopis – J Mech Eng.* 2021;71:101–8.
- [4] Muthusamy B, Chao CK, Su SJ, Cheng CW, Lin J. Effects of merged holes, partial thread removal, and offset holes on fatigue strengths of titanium locking plates. *Clin Biomech.* 2022;96:105663.
- [5] Terzini M, Aldieri A, Nurisso S, De Nisco G, Bignardi C. Finite Element Modeling Application in Forensic Practice: A Periprosthetic Femoral Fracture Case Study. *Front Bioeng Biotechnol.* 2020;8 June:1–11.
- [6] Antoniac IV, Stoia DI, Ghiban B, Tecu C, Miculescu F, Vigarú C, et al. Failure analysis of a humeral shaft locking compression plate-surface investigation and simulation by finite element method. *Materials (Basel).* 2019;12:1128.
- [7] Nakhaei M, Sterba M, Foletti JM, Badih L, Behr M. Experimental analysis and numerical fatigue life prediction of 3D-Printed osteosynthesis plates. *Front Bioeng Biotechnol.* 2023;11 March:1–13.
- [8] Bologna FA, Audenino AL, Terzini M. Bone Plates Runout Prediction Through Tensile Strength and Geometric Properties for Regulatory Mechanical Testing. *Ann Biomed Eng.* 2024;52:239–49.
- [9] Carbonaro D, Chiastra C, Bologna FA, Audenino AL, Terzini M. Determining the Mechanical Properties of Super-Elastic Nitinol Bone Staples Through an Integrated Experimental and Computational Calibration Approach. *Ann Biomed Eng.* 2024;52:682–94.
- [10] Bologna FA, Audenino AL, Terzini M. Reducing bone plates standard fatigue test time with an analytical runout load prediction. In: EIGHTH NATIONAL CONGRESS OF BIOENGINEERING. Pàtron editore; 2023. p. 1120–3.
- [11] Inacio J V., Schwarzenberg P, Yoon RS, Kantzos A, Malige A, Nwachuku CO, et al. Boundary Conditions Matter-Impact of Test Setup on Inferred Construct Mechanics in Plated Distal Femur Osteotomies. *J Biomech Eng.* 2022;144:1–11.
- [12] Bergmann G, Bergmann G, Deuretzbacher G, Deuretzbacher G, Heller M, Heller M, et al. Hip forces and gait patterns from routine activities. *J Biomech.* 2001;34:859–71.
- [13] Bologna FA, Putame G, Audenino AL, Terzini M. Understanding the role of head size and neck length in micromotion generation at the taper junction in total hip arthroplasty. *Sci Rep.* 2024;14:1–12.
- [14] Ruff CB. Mechanical determinants of bone form: Insights from skeletal remains. *J Musculoskelet Neuronal Interact.* 2005;5:202–12.
- [15] Borrelli S, Putame G, Pascoletti G, Terzini M, Zanetti EM. In Silico Meta-Analysis of Boundary Conditions for Experimental Tests on the Lumbar Spine. *Ann Biomed Eng.* 2022;50:1243–54.